The Pierre Auger Project and Enhancements

A. Etchegoyen[*,†], U. Fröhlich[**], A. Lucero[*], I. Sidelnik[*], B. Wundheiler[*]
and for the Pierre Auger Collaboration[‡]

[*]ITeDA, Instituto de Tecnologías en Detección y Astropartículas (CNEA, CONICET, UNSAM),
Argentina
[†]UTN - FRBA, Argentina
[**]Universität Siegen, Siegen, Germany
[‡]Observatorio Pierre Auger, Av. San Martín Norte 304, 5613 Malargüe, Argentina

Abstract. The current status of the scientific results of the Auger Observatory will be discussed which include spectrum, anisotropy in arrival directions, chemical composition analyses, and limits on neutrino and photon fluxes. A review of the Observatory detection systems will be presented. Auger has started the construction of its second phase which encompasses antennae for radio detection of cosmic rays, high-elevation telescopes, and surface plus muon detectors. Details will be presented on the latter, AMIGA (*Auger Muons and Infill for the Ground Array*), an Auger project consisting of 85 detector pairs each one composed of a surface water-Cherenkov detector and a buried muon counter. The detector pairs are arranged in an array with spacings of 433 and 750 m in order to perform a detailed study of the 10^{17} eV to 10^{19} eV spectrum region. Preliminary results on the performance of the 750 m array of surface detectors and the first muon counter prototype will be presented.

Keywords: Cosmic rays, galactic and extragalactic sources, Pierre Auger Observatory
PACS: 98.70.Sa, 95.85.Ry, 95.55.Vj, 95.55.Cs

INTRODUCTION

Cosmic ray observatories aim to experimentally cast light on the energy, origin, and chemical composition of the primary particles arriving to the top of the Earth atmosphere. They would generally consist on surface detectors deployed over a given area with a chosen geometry in order to reconstruct the shower lateral distribution at earth's surface (e.g. the observatory at Volcano Ranch, New Mexico where in 1962 the first air-shower with ascribed energy in excess of 100 EeV [1] was recorded). A different technique based on optical telescopes was developed and implemented by Fly's Eye/HiRes [2]. They reconstruct the longitudinal shower profile by detecting the fluorescence light produced by excitation of atmospheric nitrogen by shower electrons. Surface detectors have a 100% duty cycle and make use of simulations in order to evaluate the primary energy, while the fluorescence technique has a 10 - 15% duty cycle (clear, dark nights) and does not resort to simulations for the energy estimation, although it relies on the atmospheric fluorescence yield, on a continuous evaluation of the atmospheric light attenuation length and on the absolute calibration of the telescopes. The aperture is well defined for the surface array at higher energies while for the telescopes it increases with energy and needs to be calculated with Monte Carlo simulations. They are clearly two systems that complement each other and for this reason the Auger Observatory uses a hybrid technique with both a surface detector (SD) array and fluorescence detector (FD)

system.

As above mentioned, it is of paramount importance to measure the energy of the arriving cosmic rays. With this measurement it is possible to obtain the cosmic ray spectrum, i.e. the flux of primary particles as a function of their incoming energy.

THE COSMIC RAY SPECTRUM

The cosmic ray spectrum at higher energy only presents four distinct traits, the "knee", the "second knee", the "ankle", and the GZK cutoff and therefore a thorough understanding of cosmic rays encompasses the study of these features including their chemical composition. The knee occurs at $3 - 5 \times 10^{15} eV$ where the spectral index changes from -2.7 to -3.1 (see Fig. 1.left), the second knee at ~ 0.4 EeV (1.0 EeV = 10^{18} eV) with a further steepening of the spectrum (see Fig. 1.left), and the ankle at ~ 4 EeV (see Fig. 1.right). The GZK-cutoff (named after Greisen, Zatsepin, and Kuz'min who suggested it) is a suppression of the cosmic ray flux at very high energies [3, 4] (see Fig. 1.right) by interactions with the microwave background radiation.
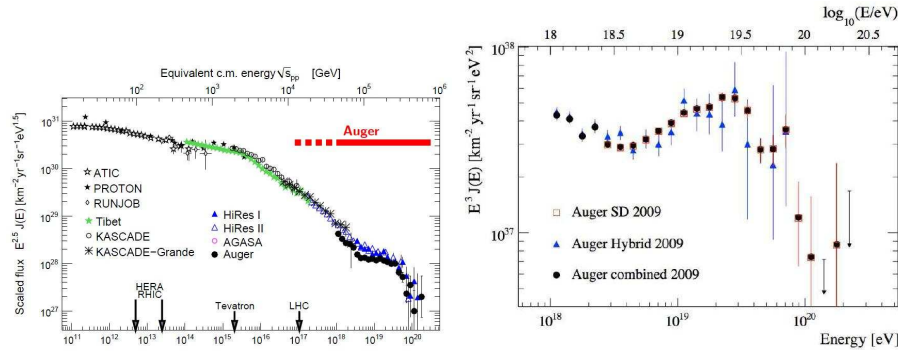

FIGURE 1. The cosmic ray spectrum; *(left)* compendium of data from different observatories with an equivalent *p-p* collider-accelerator energy scale; *(right)* Auger Observatory spectrum from SD, hybrid, and combined data [5]. Note that the flux is multiplied by E^3

The second knee was observed by AKENO [6], Fly's Eye stereo [7], and its physical interpretation is still uncertain. It might be just due to attaining the maximum cosmic rays energies within the galaxy [8] since when this limit is reached the flux will necessarily decay with a larger spectral index. Or even more, it could be the transition region from galactic to extragalactic primaries where the predominant contribution arises from extragalactic proton primaries [9, 10] due to the decreasing galactic flux.

The ankle was observed by HiRes [11] at ~ 3 EeV and by AGASA [12] but at a higher energy, ~ 10 EeV . There are two main physical interpretations of the ankle depending on where the transition from galactic to extragalactic sources takes place. If the transition occurs at the second knee, then the ankle (or the dip in the spectrum) is reported to arise from $e^- e^+$ pair production from extragalactic protons collisions with the microwave cosmic background radiation [9, 10]. On the other hand, if the transition occurs at the ankle, then the ankle would arise from the different spectrum indexes of the galactic and extragalactic components [13, 14, 15].

The red horizontal line in Fig. 1.left shows the energy range of the Auger Observatory, the full line spans the current range and the dashed line the range after the enhancements which are currently being installed. The most relevant scientific results of Pierre Auger Observatory will be presented after a short outline of the Observatory detection systems that will help to assess the data quality. Finally the current Observatory upgrades and their prospective science will be described.

THE PIERRE AUGER OBSERVATORY

The Pierre Auger Project [16] studies the highest energies cosmic rays arriving on the surface of the earth from outer space. It aims at building two Observatories situated in both hemispheres and in November 2008 the austral observatory in Malargüe, Province of Mendoza, Argentina was formally inaugurated. The Collaboration now focusses on the construction of Auger North [17, 18] in Colorado, USA, which is designed to have a much larger acceptance in order to significantly enhance the study cosmic rays with energies above ~ 60 EeV.

The Auger observatory has two distinctive features: its exceptional size and its hybrid nature (i.e. both surface detector [19] and fluorescence [20] telescope systems). As such, Auger provides a large number of events with better controlled systematic detection uncertainties.

The SD array consists of 1600 cylindrical water Cherenkov detectors of 10 m$^2 \times$ 1.2 m high arranged on a triangular grid with 1.5 km spacing, covering an area of 3000 km^2 at $\sim$ 1400 m above sea level. The principle of operation of these detectors is that charged particles produce Cherenkov light when traversing the 12 tons of pure water lodged in the tank. This light is partially collected by three symmetrically placed 9" photomultiplier tubes (PMT) at the water surface, placed 1.2 m away from the tank center.

The FD system was originally designed to be constituted by 24 telescopes, deployed in 4 buildings hosting 6 telescopes each overlooking the SD array (see Fig. 2.left). Each telescope has an optical filter and corrector ring at the entrance window, a mirror and a PMT camera on its focal plane where the fluorescence light is collected. This system produces a light spot with a $0.5°$ spread while each PMT has a FOV (Field of View) of $1.5°$.

As mentioned already, the Observatory aims to study the energy, origin and chemical composition of the primary particle. The origin is studied by extrapolating back the reconstructed arrival directions and the composition by measuring the atmospheric depth where showers have their maximum development, X_{max} [21]. The energy calibration is dominated by FD systematic uncertainties with a total estimated value of 22 % [22], the arrival direction uncertainty is better than 1.0% for primaries with energy above 10 EeV [23], and the X_{max} uncertainty is 20 g/cm^2 [21].
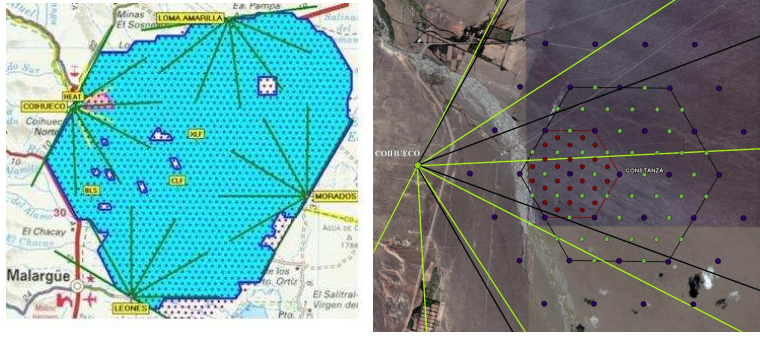
FIGURE 2. Layout of the Auger Observatory, green lines limit the FOV of the 6 telescopes with $1.5° - 30° \times 0° - 30°$ elevation and azimuth FOV. *(left)* Dots symbolize SD positions, those in the blue shaded area are operational; *(right)* layout of the Auger Observatory upgrades near Cerro Coihueco. Black lines limit the $30° - 58° \times 0° - 30°$ FOV for the 3 HEAT telescopes. The two hexagons limit the AMIGA infilled areas of 5.9 and 23.5 km^2 with 433 and 750 m triangular grid detector spacings, respectively. Each dot within these hexagons represents a pair of a water Cherenkov detector and a muon counter. The center dot, named Constanza, is placed ~ 6.0 km away from Cerro Coihueco.

SCIENTIFIC RESULTS OF THE PIERRE AUGER OBSERVATORY

The most prominent scientific results obtained by the Pierre Auger Observatory will now be outlined.

End of the Spectrum. The cosmic ray flux was measured with both hybrid and SD array data [5] showing a good agreement. A combined spectrum has been derived with high statistics covering the energy range from 1.0 to above 100 EeV (see Fig. 1.right) with an estimated energy systematic uncertainty of 22%. The ankle was found at $log_{10}(E_{ankle}/eV) = 18.61 \pm 0.01$. The spectrum is suppressed at $log_{10}(E_{1/2}/eV) = 19.61 \pm 0.03$ with a significance in excess of 20 σ.

Anisotropy. The last update on anisotropy data of correlations between the arrival directions of the highest energy cosmic rays and the positions of nearby objects is discussed elsewhere ([24, 25]). Events above 55 EeV were selected and 17 out of 44 correlate with the position of nearby objects from the Véron-Cetty and Véron (VCV) catalog. The cumulative binomial probability that an isotropic flux leads to 17 or more correlations is low, 0.006. Still, this correlation is weaker than the one published in an earlier analysis [26].

Shower Depth of Maximum. The analyses of the X_{max} and rms(X_{max}) measured values are shown and discussed in [21]. They support the hypothesis that the transition from galactic to extragalactic cosmic rays occurs in the ankle region. Moreover and assuming that the hadronic interaction properties do not change much within the observed energy range, both the observed X_{max} and their fluctuations independently are a signature of an increasing average mass of the primary particles with energy up to 59 EeV, which is of interest to analyze in contrast to the anisotropy results (though in a higher energy region) since the latter tends to imply a lighter composition, i.e. protons. Heavier primaries will

have a larger deflection in the galactic and intergalactic magnetic fields, thus preventing the correlation with point sources. Maybe the hadronic interactions change in this energy range and as such further studies might cast light on them.

Photon Limits. No high-energy photons were identified and the derived upper limits are discussed in [27]. The results complement the previous constraints on top-down models from Auger surface detector data. In future photon searches, the separation power between photons and nuclear primaries can be enhanced by adding information for the Auger Observatories upgrades (see below).

Tau Neutrino Limit. Data was analyzed to present an upper limit to the diffuse flux of ν_τ [28], no neutrinos were detected yet although the Auger Observatory has the best detection sensitivity currently available around a few EeV, which is the most relevant energy to explore the predicted fluxes of GZK neutrinos. However in the worst case of systematic uncertainties, the limit presented here is still higher by about one order of magnitude than GZK neutrino predictions and as such more data needs to be collected to make a final assessment.

UPGRADES OF THE PIERRE AUGER OBSERVATORY

It is of uppermost relevance to study the 0.1 - 10 EeV energy range in order to cast light on the second knee and ankle features. The two main requirements are good energy resolution and primary type identification (statistical discrimination over this energy range will suffice) since as mentioned above the transition from galactic (heavier elements) to extragalactic (lighter elements) sources is directly linked to primary composition.

The two shower parameters relevant to composition are the atmospheric depth at shower maximum, X_{max}, and the shower muon content. Composition is very poorly understood in this energy range where varieties of mixed compositions are reported ranging from proton to iron dominated primaries (see [29] and references within). Still, composition can only be assessed within a given hadronic interaction model and therefore comparisons are only to be performed under those premises. Moreover, they would need a recalculation if a hadronic model is reformulated. Much more robust results are attained from the variation rate of either X_{max} (called elongation rate) or muon content as a function of energy [30] by which composition changes may be assessed fairly independent of the assumed hadronic model.

The Auger Observatory is being upgraded to study the primary particle type in the second knee - ankle region with both fluorescence telescopes and muon counters (MC) giving the air shower longitudinal profiles and muon contents, respectively. It will therefore perform spectrum and composition measurements with unprecedented accuracy.

Within the original Auger baseline design, the surface array is fully efficient above $\sim$ 3 EeV and in the hybrid mode this range is extended down to $\sim$ 1 EeV. There are three enhancements to make the Observatory fully efficient down $\sim$ 0.1 EeV: HEAT (*High Elevation Auger Telescopes*) [31, 32], AMIGA (*Auger Muons and Infill for the Ground*

Array) [33, 34, 35, 36], and AERA (*Auger Engineering Radio Array*) [37]. Moreover, these enhancements focuss on composition analyses.

HEAT. HEAT adds to the Observatory three new telescopes of similar design to the previous ones in order to fully detect longitudinal profiles of showers in the $1.5° \times 58°$ elevation range. The original telescopes cover the range of $1.5° \times 30°$ while the HEAT telescopes $30° \times 58°$. This is attained by tilting the telescopes enclosures upwards by 29° (see Fig. 3.left). This higher elevation FOV is needed for the detection of lower-energy showers since they would develop earlier in the atmosphere and they have to be detected at closer distances because the fluorescence light produced is roughly proportional to the primary energy. HEAT is already taking data and a reconstructed longitudinal profile of a low energy event is displayed in Fig. 3.right.
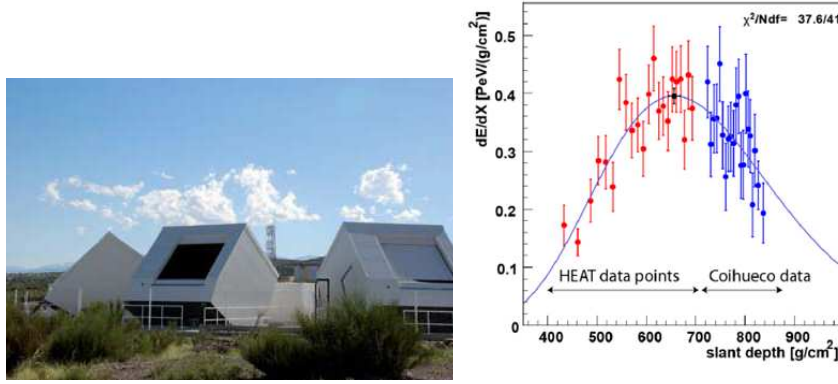

FIGURE 3. *(left)* The three buildings of the HEAT telescopes at Cerro Coihueco; *(right)* longitudinal shower profile where both HEAT and Coihueco telescopes are needed in order to reconstruct the profile, event energy $(2.0 \pm 0.2)10^{17}$ eV.

HEAT is optimized to record nearby showers in combination with the existing telescopes at Coihueco as well as to take data with AMIGA. The first measurements have showed that HEAT will improve the energy threshold down to 0.1 EeV and that the operation fulfills the design requirements.

AMIGA. AMIGA is being deployed over a small graded infilled area of 23.5 km^2 (see Fig. 2.right) since the cosmic ray flux rapidly increases as the energy threshold is lowered. On the other hand, the detectors have to be deployed at shorter distances among each other in a denser array since lower energies imply smaller airshower footprints on the ground. A graded infill of 433 and 750 m triangular grids was chosen in order to optimize the detection over more than an order of magnitude, from 3 EeV down to 0.1 EeV. Also, and since the two main experimental requirements of the new detection system are good energy resolution and primary type identification, AMIGA consists of pairs of water Cherenkov surface detectors and muon counters over viewed by FDs. It entails 85 of such pairs (Fig. 4.left).

Deployment begins with an engineering array called Unitary Cell, a hexagon with 7 detector pairs, one in each hexagon vertex and one in the center. These counters are composed of 4 modules each, 2×5 m^2 and 2×10 m^2 with 2 and 4 m long strips, respectively. Each counter has an area of 30 m^2 and it is made of 4 modules of 64

scintillator strips each, 32 on each side of the PMT, (see Fig. 4.right) with glued optical fibers (doped with wave length shifters) in a groove coated on top with a reflective foil. The strips are 1 cm thick and 4.1 cm wide.
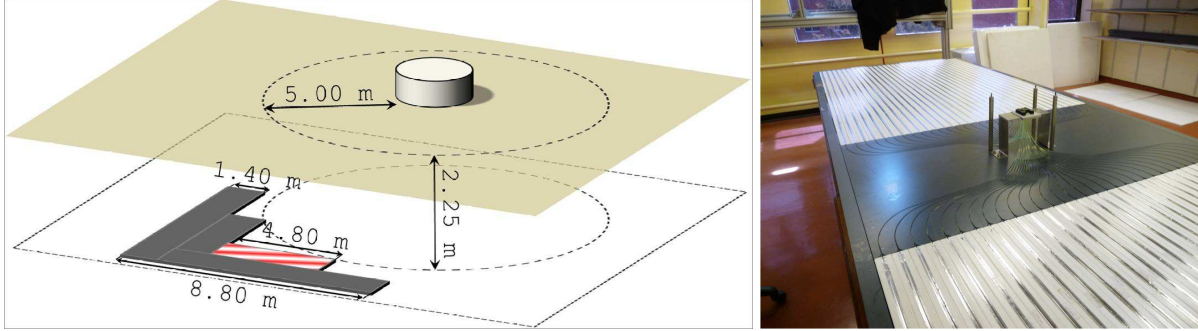

FIGURE 4. *(left)* Layout of the SD-MC doublet, a 5 m^2 module depicted with red strips; *(right)* first 5 m^2 prototype, scintillator strips layout and fiber routing onto the optical connector.

Each module has a 64 pixel high quantum efficiency Hamamatsu H8804MOD PMT with a 2 mm × 2 mm pixel size. Since the PMT is the counter sensitive element, its performance parameters need to be known, assessed, and set (see e.g. Fig. 5.left) in order to ensure its proper functioning for data acquisition. Therefore, each AMIGA PMT will be analyzed by a test facility designed and built for this purpose.

The front end bandwidth is of 180 MHz and the electronics sampling is performed at 320 MSps (3.125 ns) with an external memory to store up to 6 ms of data, equivalent to 1024 showers. The total number of independent electronic channels per counter is 256. This high segmentation requirement is an attempt to measure a single muon per segment per unit time in order to avoid pile-up. A signal is counted as a muon if it has two or more single photo electrons (spe). In turn, an spe is registered when its amplitude is above ∼ 30 % of each pixel mean spe value. The counter so designed is very robust and trustworthy because obtaining the muon number from the integrated signal has significant disadvantages: i) the number of spe per muon vary as much as a factor of ∼ 2 due to fiber attenuation depending on whether the muon arrives at the near or far end of the scintillator strip (see Fig. 5.righ), ii) the light yield from the same fiber type may vary a factor of ∼ 1.5 , and iii) changes in gain or in spe numbers will impact on the muon counting via total charge collected.

The first fully equipped 5 m^2 prototype module has been designed, built, tested, and buried at the Observatory site in November 2009 (see Fig.6), depicted in red strips in Fig. 4.left.

Data have been taken with this 5 m^2 prototype counter by requiring at least 8 channels to simultaneously trigger in any given time bin of 12.5 ns. A typical time structure of an event is shown in Fig. 7.left.

Also 50/61 SDs of the 750 m infilled area are now operational and, in particular, the 7 SDs of the unitary cell have been instrumented with the new telecommunication system designed and built for AMIGA (industrial grade radios XBee Pro working over IP and using the IEEE 802.15.4 standard controlled with a local TS7260 single board microcomputer). The graded infill was envisaged to have both a saturated efficiency down to 0.1 EeV and as a by-product to experimentally test the main array reconstruction
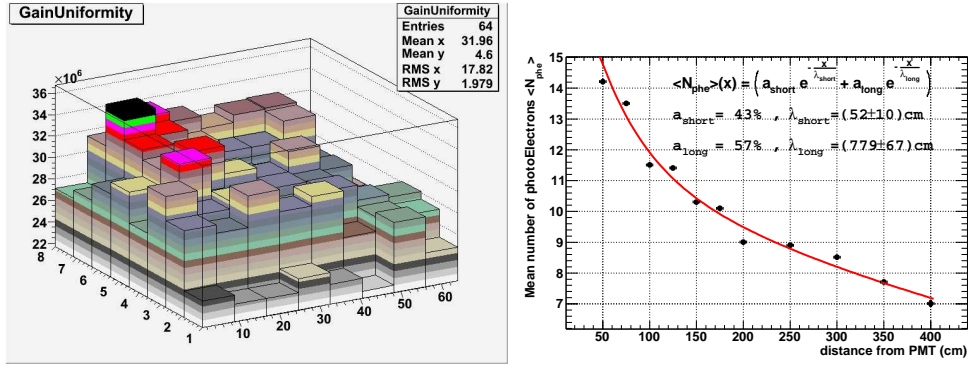
FIGURE 5. *(left)* gain uniformity of an 8×8 pixel Hamamatsu H8804MOD PMT; *(right)* light attenuation of a 1.2 mm Kuraray optical fiber, light produced by background muons traversing a scintillator strip.

FIGURE 6. *(left)* First module buried at the Observatory site, the insert shows the electronics inside its enclosure; *(right)* module in the well placed over a sand bed with service pipe installed, about to be buried.
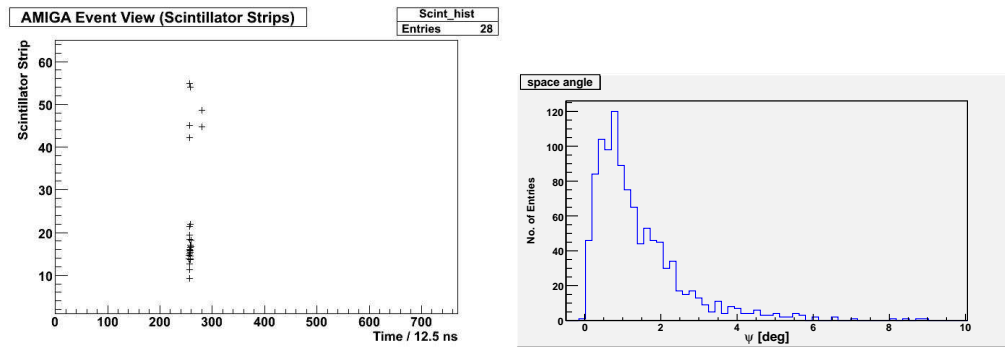

FIGURE 7. *(left) A typical event recorded by the prototype module. On the horizontal axis is the time in units of 12.5 ns and on the vertical axis the scintillator strip number. Twelve strips triggered, all in the same time bin (# 256); (right) histogram of the difference in the reconstruction of arrival directions with and without the infill SDs.*

uncertainties. Preliminary tests have been performed by the reconstruction of events with and without the infill SDs with a data set with ≥ 7 and ≥ 3 or more SDs for the infilled and main arrays, respectively [34, 38]. One of such a tests, a comparison of the arrival directions, resulted in an upper limit $1.4°$ (see Fig. 7.right). This shows the good performance of the main array even with a reduced number of triggered stations and below its 3 EeV lower energy threshold limit.

AERA. AERA aims at the detection of cosmic-ray showers by measuring the coherent radiation at radio frequencies emitted by secondary particles, which are deflected by the geomagnetic field. The radio-detection technique has been investigated already in the 1960's (see e.g. [39]) and results from more recent experiments at energies beyond 10^{17} eV (LOPES [40] and CODALEMA [41]) show the great potential of this technique. The main advantages of radio detection are a nearly 100% duty cycle, a signal to noise ratio scaling with the square of the cosmic-ray energy, and its high angular resolution and sensitivity to the longitudinal air-shower evolution. These features, combined with the capability of measuring the depth at shower maximum (composition analysis) and the cost effectiveness for instrumentation in large arrays, makes it an excellent complement to the Auger SD array.
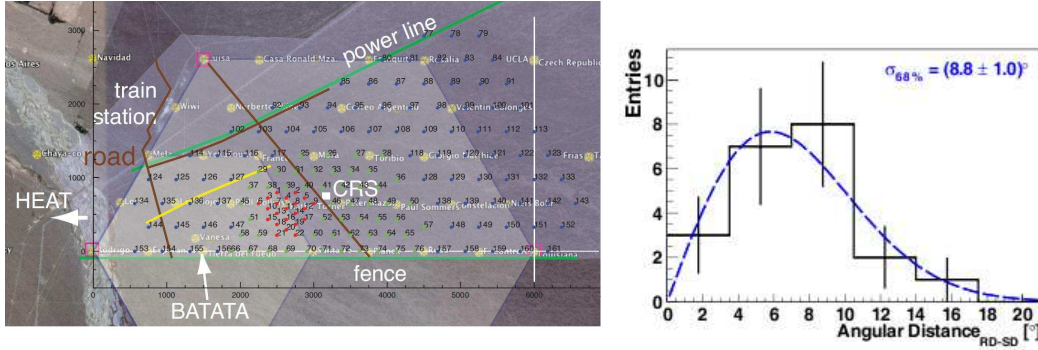

FIGURE 8. *(left)* Layout of the proposed AERA graded array overlaying the AMIGA hexagons in the background. The location of each antenna is marked as a red box; *(right)* a preliminary comparison of reconstructed arrival directions with both SD and radio stations; the angular resolution of these initial measurements was dominated by timing resolution of the detector stations (see [42] for more details).

AERA is composed of 150 self-triggered radio-detection stations over ~ 20 km^2 [37] and it is now being deployed in the AMIGA-HEAT region (see Fig. 8.*left*). It consists of a graded infilled area with different station densities in order to cover a large energy region above 0.1 EeV. Primary energies, types, and arrival directions (see a preliminary result in Fig. 8.*right*) will be reconstructed by super-hybrid measurements entailing four totally independent measuring systems, SD, FD, MC, and radio-detection antennae.

In conclusion, the Auger Observatory has measured the high energy cosmic ray spectrum and clearly identified the ankle and the cutoff, it also found clear indications of anisotropy in the arrival directions of cosmic rays with energies above 55 EeV. Statistical composition analyses have been performed with depths at shower maximum and their fluctuations which merit further research particularly in hadron interactions at higher energies. New upper limits have been found for photon and tau neutrino fluxes. Enhancements are well under way in order to study the transition region from galactic

to extragalactic sources with surface detectors, optical telescopes, muon counters and radio-detection antennae with unitary efficiencies unbiased in composition.

REFERENCES

1. J. Linsley, J., *Catalog of Highest Energy Cosmic Ray*, edited by M. Wada (World Data Center of Cosmic Rays, Institute of Physical and Chemical Research, Itabashi, Tokyo), Vol. 1, p. 1. (1980).
2. R.M. Baltrusaitis et al., *Nucl. Inst. & Meth.*, **A240**, 410, (1985).
3. K. Greisen, *Phys. Rev. Lett.* **16**, 748, (1966).
4. G.T. Zatsepin, V.A. Kuzmin, *Sov. Phys. JETP Lett.*, **4**, 78, (1966).
5. The Pierre Auger Collaboration, *Phys. Letts.* **B**, 685, 239-246, (2010).
6. Nagano M. et al., *J. Phys. G* **18**, 423,(1992).
7. Bird D. J. et al., *Phys. Rev. Lett.* **71**, 3401, (1993).
8. A. Haungs et al. (KASCADE-Grande Coll.), *astro-ph*/0508286.
9. V.S. Berenzinsky et al. *Phys. Lett. B* **612**, 147, (2005) and *astro-ph*/0502550.
10. V.S. Berenzinsky, *astro-ph*/0509069.
11. R. U. Abbasi et al. (HiRes Collab.), *Astropart. Phys.* **32**, 53-60, (2009).
12. M. Takeda et al., *Astropart. Phys.* **19**, 447, (2003).
13. A.M. Hillas, *Nucl. Phys. B (Proc. Suppl)* **136**, 139, (2004).
14. T. Wibig y A.W. Wolfendale, *J. Phys. G* **31**, 255, (2005).
15. D. Allard et al., *astro-ph*/0505566.
16. The Auger Collaboration, *Nucl. Inst. & Meth.*, **A523**, 50-95, (2004).
17. J. Bluemer for the Pierre Auger Collaboration, *New Journal of Physics* (2010), accepted.
18. D. Nitz for the Pierre Auger Collaboration, Proceeding of the 12th Vienna Conference on Instrumentation, (2010), to be published.
19. I.Allekotte et al., *Nucl. Inst. and Meths.* **A**, 409–420 (2008).
20. The Pierre Auger Collaboration, submitted to *Nucl. Inst. and Meths.* **A**, (arXiv:0907.4282v1 [astro-ph.IM]).
21. The Pierre Auger Collaboration, *Phys. Rev. Letts* **104**, 091101, (2010).
22. M. Platino for the Pierre Auger Collaboration, 2009, Proc. 31st ICRC (Lodz, Poland), #0142.
23. C. Bonifazi for the Pierre Auger Collaboration, *Nuclear Physics* **B** (Proc. Suppl.),2009, 190, 20-25; arXiv:0901.3138v1 [astro-ph.HE]
24. J.D. Hague for the Pierre Auger Collaboration, 2009, Proc. 31th ICRC (Lodz, Polonia), #0143.
25. The Auger Collaboration, manuscript in progress.
26. The Pierre Auger Collaboration, *Science***318** 939, (2007).
27. The Pierre Auger Collaboration, *Astropart. Phys.* **31**, 399-406, (2009).
28. The Pierre Auger Collaboration, *Phys. Rev.* **D79**, 102001, (2010).
29. L. Anchordoqui et al., *hep-ph*/0407020.
30. T. Abuy-Zayyad et al., *Phys. Rev. Letts.* **84**, 4276-4279 (2000).
31. H. Klages for the Pierre Auger Collaboration, 2007, Proc. 30th ICRC (Mérida-México), #0065.
32. M. Kleifges for the Pierre Auger Collaboration, 2009, Proc. 31st ICRC (Lodz, Poland), #0410.
33. A. Etchegoyen for the Pierre Auger Collaboration, 2007, Proc. 30th ICRC (Mérida-México), #1307.
34. M. Platino for the Pierre Auger Collaboration, 2009, Proc. 31st ICRC (Lodz, Poland), #0184.
35. P. Buchholz for the Pierre Auger Collaboration, 2009, Proc. 31st ICRC (Lodz, Poland), #0043.
36. G. Medina-Tanco for the Pierre Auger Collaboration, 2009, Proc. 31st ICRC (Lodz, Poland), #0137.
37. A. M. van der Berg for the Pierre Auger Collaboration, 2009, Proc. 31st ICRC (Lodz, Poland), #0232.
38. I.P. Sidelnik, G. Navarra, and A. Etchegoyen, Pierre Auger Project internal note, 2009, #111.
39. J. V. Jelley, J. H. Fruin, N. A. Porter T. C. Weekes, F. G. Smith & R. A. Porter, *Nature* **205**, 327 - 328 (1965)
40. A. Haungs, *Nucl. Instr. and Meth. A* (2009), doi:10.1016/j.nima.2009.03.033.
41. P. Lautridou et al., *Nucl. Instr. and Meth. A* (2009), doi:10.1016/j.nima.2009.03.164.
42. J. Coppens for the Pierre Auger Collaboration, *Nucl. Instr. and Meth. A* (2009) doi:10.1016/j.nima.2009.03.119